



Metal-Based Drugs

Synthesis and Mode of Action Studies on Iridium(I)–NHC Anticancer Drug Candidates

Yvonne Gothe,^[a] Isolda Romero-Canelón,^[b] Tiziano Marzo,^[c,d] Peter J. Sadler,^[e] Luigi Messori,^[c] and Nils Metzler-Nolte*^[a]

Abstract: We report the synthesis, characterization, and biological activity of Ir^I complexes with triazole- (NNHC) and thiazole-based (NSHC) N-heterocyclic carbene ligands. Starting from the dimeric [Ir(COD)Cl]₂, we obtained complexes of composition Ir(COD)(NNHC)Cl (**4a**), Ir(COD)(NNHC)X (**4b**: X = Cl; **4bBr**: X = Br), [Ir(COD)(NNHC)(NHC)]I (**5a**), [Ir(COD)(NSHC)₂]Cl (**6a**), and [Ir(COD)(NSHC)(NNHC)]Cl (**6b**) by adaptation of established synthetic methods for metal–NHC complexes. Their interactions with model proteins cytochrome c and lysozyme, as well as with the oligonucleotide hexamer (CG)₃ (ODN1), were studied.

Although most complexes did not show any strong interactions with these biomolecules, all complexes were active against HT-29 and MCF-7 cancerous cells, with IC₅₀ values ranging between 1 and 60 μm. The most active compounds were the cationic bis(carbene) derivatives **5** and **6**. All compounds generated high levels of reactive oxygen species (ROS) after incubation for 48 h in MCF-7 cells, possibly suggesting a redox-mediated mechanism of action. Interestingly, there were distinctive differences in the superoxide/(total ROS) ratios induced by the different groups of compounds.

Introduction

The field of medicinal inorganic chemistry arguably originates from the success of the clinical Pt-based anticancer complexes, most importantly cisplatin. Numerous studies have investigated the mode of action of this important inorganic compound in impressive detail.^[1] Inspired by this work, complexes from metals other than Pt were investigated for their antiproliferative activity. Many of those are indeed organometallic compounds,^[2] and Ir compounds in particular have gained significant attention recently. Iridium, in its two biologically-relevant oxidation states +I and +III, has some attractive features. For example, Ir^{III} with the d⁶ electronic configuration has excellent luminescent properties, which have been exploited for cellular imaging by Lo and others.^[3] Perhaps surprisingly, organometallic Ir^{III} half-sandwich complexes with cyclopentadienyl (Cp) ligands exhibit a wide range of ligand substitution rates, depend-

ent on the nature of the other ligands. Some are very stable under biological conditions and ligand exchange is remarkably slow, reminiscent of the relatively slow chloride-to-water exchange in cisplatin, but others can exchange ligands on a much faster timescale. Octahedral and pseudo-octahedral Ir^{III} compounds have been comprehensively investigated for their antiproliferative activity.^[4] Ir^I, on the other hand, has a d⁸ electronic configuration, identical to Pt^{II} compounds, with similar square-planar geometry. Unlike Pt^{II}, however, Ir^I compounds are readily oxidized to Ir^{III} derivatives. This redox chemistry is elegantly used in Ir-based catalytic metallodrugs, as investigated by the groups of Sadler, Liu, and others recently.^[5,6] There is, however, only a handful of studies on the biological activity of Ir^I compounds.^[7]

With respect to Ir^I-based compounds, most notable is the lack of knowledge concerning their interactions with biological systems. We have investigated the antiproliferative activity of Ir^I compounds with cyclooctadiene (COD) and N-heterocyclic carbene (NHC) ligands. In these studies, we found that these complexes bind to model proteins such as cytochrome c through an unusual oxidative mechanism, in that Ir^I becomes oxidized to Ir^{III}, which causes irreversible binding to protein targets and might thus be responsible for the good activity of the Ir^I compounds.^[7c] However later, we discovered that cationic Ir^I-bis(carbene) complexes do not readily bind to proteins by this mechanism, but still exhibit even greater antiproliferative activity.^[7e]

To further investigate these seemingly contradictory findings, we have now prepared a number of new Ir^I complexes with different carbene-type ligands beyond the prototypical N-heterocyclic Arduengo carbenes, and have investigated their antiproliferative behavior as well as binding to model proteins

[a] *Inorganic Chemistry I – Bioinorganic Chemistry, Faculty of Chemistry and Biochemistry, Ruhr-University Bochum, Universitätsstrasse 150, 44801 Bochum, Germany*
E-mail: nils.metzler-nolte@rub.de
www.chemie.rub.de/ac1

[b] *School of Pharmacy, Institute of Clinical Sciences, University of Birmingham, Birmingham B15 2TT, UK*

[c] *Department of Chemistry, University of Florence, Via della Lastruccia 3, 50019 Sesto Fiorentino, Italy*

[d] *Department of Chemistry and Industrial Chemistry (DCCI), University of Pisa, Via Moruzzi 13, 56124 Pisa, Italy*

[e] *Department of Chemistry, University of Warwick, Coventry CV4 7AL, UK*

Supporting information and ORCID(s) from the author(s) for this article are available on the WWW under <https://doi.org/10.1002/ejic.201800225>.

and DNA. In addition – noting the possibility of catalytic redox cycling between Ir^I and Ir^{III} – the possible involvement of ROS (reactive oxygen species) in their mechanism of action was investigated.

Results and Discussion

Synthesis and Characterization

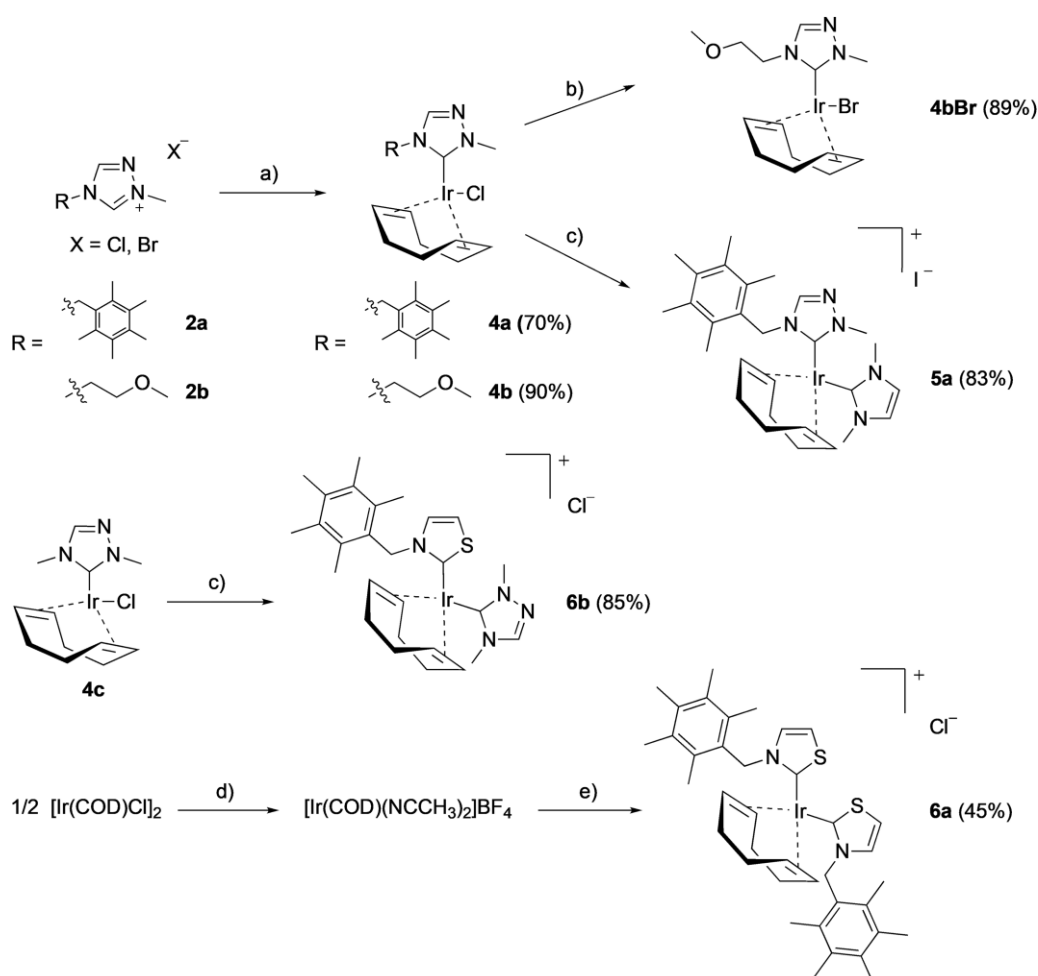
The synthesis of the iridium complexes studied in this work is summarized in Scheme 1. The compounds consist of different heterocyclic ligand systems which are imidazole (NHC), triazole (NNHC) and thiazole (NSHC). In our previous work, we showed that a high lipophilicity of Ir^I carbene complexes has a positive impact on the compounds' antiproliferative activity.^[7e] For this reason, we decided to N-substitute the NHC-type ligands used in this work with pentamethyl-benzyl side-chains as well.

All ligands were prepared according to well-established procedures starting from 1-methyl-1,2,4-triazole or thiazole via an alkylation reaction (Menschutkin reaction) of the second aromatic nitrogen.^[8] Compounds **2a**, **b** and **3a** were obtained by reacting 1-methyl-1,2,4-triazole (**2a**, **b**) or thiazole (**3a**) with

1 mol equivalent of the respective alkyl halide in either THF or acetonitrile for 48–96 h. 1,4-Dimethyl-4*H*-1,2,4-triazolium iodide (**2c**) formed within 5 min in the absence of any solvent, as indicated by precipitation of the compound. NMR spectra of the ligands showed the expected signals. For all ligands, the fragment [M – X]⁺ with (X = Cl, Br, I) is observed by mass spectrometry (ESI-MS, positive ion detection mode), due to the positive charge of these organic ligands.

The monocarbene complexes **4a**, **b** were obtained by a transmetalation reaction from the corresponding silver carbene derivatives by a two-step synthesis following previously described procedures.^[7e] The silver carbene complexes were generated in situ by treatment of the respective triazolium salts with half an equivalent of Ag₂O. The addition of [Ir(COD)Cl]₂ led to the corresponding iridium complexes **4a** and **4b** (Scheme 1).

Compound **4bBr** was obtained by simply exchanging the chlorido ligand in **4b** with bromide by stirring **4b** with an excess of KBr in acetonitrile. The successful exchange was proven by FAB⁺-MS, which shows the M⁺ peak in each case. Furthermore, small changes in the chemical shifts of the olefinic COD carbon atoms in the ¹³C NMR and of the methyl group in the ¹H NMR spectrum are observed.



Scheme 1. (a) 0.5 equiv. Ag₂O, 0.5 equiv. [Ir(COD)Cl]₂, CH₂Cl₂, room temp. overnight, (b) 3 equiv. KBr, acetonitrile, r.t. overnight, (c) **1/3a** respectively, 1 equiv. K₂CO₃, CH₂Cl₂, r.t., 2–5 d, (d) NaBF₄, acetonitrile, r.t., (e) **3a**, KOtBu, r.t., overnight.

The synthesis of bis(carbene) complexes such as **7** (Figure 1) containing two NHC ligands has been described in previous work.^[7e] The bis(carbene) complexes **5a** and **6b** were prepared in the same way as **7** by reacting the monocarbene complex with the corresponding imidazolium/thiazolium salt in the presence of a mild base. Herein, the reaction time strongly depends on the steric demand of the N-substituent. Eventually, also these complexes were obtained in high purity and very good yields. NMR spectroscopy and mass spectrometry confirmed the successful formation of the complexes including the characteristic appearance of a second carbene signal in the ¹³C NMR spectra.

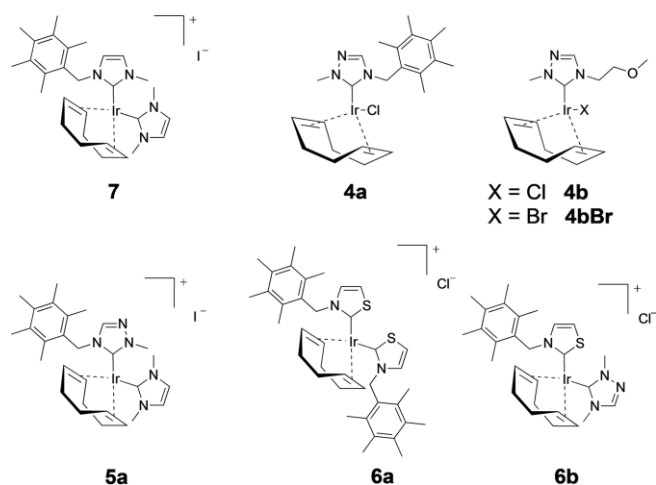


Figure 1. Chemical structures of the investigated Ir complexes.

The synthesis of a bis(carbene) complex of the type $[\text{Ir}(\text{NSHC})_2(\text{COD})]\text{X}$ was challenging since all efforts to synthesize the Ir^I-NSHC monocarbene complexes remained ineffective. A first test reaction for a monocarbene iridium complex composed of a thiazole ligand was undertaken with thiazolium salt **3a** under the very same conditions as for the monocarbene complexes **4a, b** using Ag_2O and $[\text{Ir}(\text{COD})\text{Cl}]_2$. After stirring for 24 h followed by the established work-up procedure, the target complex could not be obtained, neither by changing solvent, temperature or increasing reaction time. The most obvious explanation is a reaction of silver with sulfur, since this problem did not occur for the respective iridium complexes with imidazole- and triazole ligands. Consequently, a second attempt was made by using $[\text{Ir}(\text{COD})\text{OMe}]_2$ as iridium precursor and base at the same time, thus avoiding the presence of silver ions. Unfortunately, the desired product was not obtained. The synthesis of thiazole-based Ir^I-carbene complexes appears to be a prevalent problem, corroborated by a few reports in the literature.^[9] In 2006, Huynh et al. published a synthesis for Ir^I-carbenes with a benzothiazolin-2-ylidene ligand yielding the desired Ir^I-NSHC monocarbene complex. Therein, the successful formation was achieved via precoordination of an *N*-allyl substituent of the ligand to the $[\text{Ir}(\text{COD})(\text{NCCH}_3)_2]\text{BF}_4$ precursor and subsequent deprotonation at the C2 position by addition of a base. The successful synthesis of the Ir^I-NSHC bis(carbene) complex **6a** was finally accomplished by slightly changing the syn-

thesis procedure mentioned above. $[\text{Ir}(\text{COD})(\text{NCCH}_3)_2]\text{BF}_4$ was synthesized by treating $[\text{Ir}(\text{COD})\text{Cl}]_2$ with sodium tetrafluoroborate in acetonitrile resulting in the replacement of both chlorido ligands by the more labile acetonitrile ligand. Subsequent addition of thiazolium salt **3a** and KO^tBu led to the desired bis(carbene) complex **6a** of the type $[\text{Ir}(\text{NSHC})_2(\text{COD})]\text{Cl}$.

This complex was characterized by ¹H/¹³C NMR and ESI-MS confirming its identity and purity. The ³J_{H4-H5} coupling constant of 3.9 Hz is comparatively large and is attributed to the strong influence of the sulfur atom. The ¹³C NMR signal of the carbene carbon atom is observed at $\delta = 206.1$ ppm and is consequently strongly shifted to lower field compared to its triazole analogues. The same observation was made for complex **6b**. Interestingly, stirring a solution of **6a** and triazolium salt **2c** led to the complete exchange of the thiazole carbene ligands by the triazole carbene ligands. This relatively low stability of the thiazole carbenes was affirmed by initial stability studies (see below).

Antiproliferative Activity

To evaluate the suitability of the new iridium complexes as anti-cancer drug candidates, their in vitro antiproliferative effects were studied on two well-established cancer cell lines that are commonly used for a first screening: HT-29, which is a human colorectal adenocarcinoma cell line and MCF-7, a human cell line from breast adenocarcinoma with low metastatic potential. These studies were performed with an incubation time of 48 h using the cell-based MTT assay. Stock solutions of the compounds were prepared in DMSO, due to poor water solubility of the monocarbene complexes. Since DMSO itself may impact on the proliferation, final DMSO concentrations of 0.5 % were used for concentrations up to 100 μM . In addition, the use of a concentration of 0.5 % DMSO was extended to all complexes even with higher water solubility, in order to guarantee a valid comparison between the different classes of compounds. Figure 1 gives an overview of the investigated complexes.

All complexes show antiproliferative effects against the two representative cancer cell lines. The antiproliferative activity of the bis(carbene) complexes **5a, 6a** and **6b** and **7**^[7e] in the high nanomolar range is notably higher (Table 1), whereas the antiproliferative activity of the monocarbene complexes lies in the low micromolar range with similar activities for MCF-7 and HT-29 cells ranging from 10.3 to 63 μM . This behavior is in accordance with previous results that we obtained for a series of mono- and bis(carbene) complexes with imidazole-based li-

Table 1. Antiproliferative effects of the complexes [$\mu\text{M} \pm \text{SD}$]. Numbers are reported to two relevant digits in all cases for consistency, thus resulting in apparently different precision.

Complex	MCF-7	HT-29
7	0.54 ± 0.27 ^[7e]	0.470 ± 0.063 ^[7e]
4a	10.3 ± 2.9	17.2 ± 2.8
4b	35 ± 6	63 ± 10
4bBr	44 ± 10	53 ± 9
5a	1.5 ± 0.2	1.5 ± 0.3
6a	0.92 ± 0.06	0.9 ± 0.2
6b	1.0 ± 0.3	0.9 ± 0.2

gands where the introduction of a second carbene ligand significantly increased the antiproliferative activity.^[7e] It is nonetheless remarkable, as the neutral monocarbene complexes tend to be more lipophilic than the cationic biscarbenes, and thus their cellular uptake can be assumed to be higher.

Among the monocarbene complexes **4a**, **4b** and **4bBr**, the highest antiproliferative activity is observed for **4a** with three times lower IC₅₀ values. This could be due to the more lipophilic ligand side chain of **4a** which might be related to a better cellular uptake. Different from other compound classes, the effect of the substitution of the chlorido ligand by an bromido ligand in the case of **4b/4bBr** is negligible.

Complex **7** possesses the highest activity among all bis(carbene) complexes. However, only small differences are noticed between IC₅₀ for members of this compound class, in the range of 1 μ M. With regard to the cell lines used, no general selectivity toward MCF-7 or HT-29 cells is observed.

Reactivity with Proteins

In order to investigate the interactions of the compounds with proteins, metalation studies were systemically carried out on horse heart cytochrome c and hen egg white lysozyme as two model proteins. The interaction between these proteins and the metal complexes has been studied using high-resolution electrospray ionization mass spectrometry (HR-ESI-MS), a widely used tool for studying the interactions of metallodrugs with biomolecules.^[10]

The complexes were generally dissolved in ammonium acetate buffer [10 % DMSO for the bis(carbene) complexes (30 % DMSO for **6a**) and 50 % DMSO for all monocarbene complexes] and incubated with the protein (3:1 and 10:1 complex/protein ratio) at 37 °C. At selected time points (24 h, 48 h and 72 h), aliquots were analyzed by HR-ESI MS. Unambiguous differences

in the metalation behavior were observed for the different classes of compounds.

For complexes **4** (Figure 1), we could detect ions that correspond to Ir(NHC) metal fragments binding to the respective proteins, after loss of the COD and halide ligands and oxidation to Ir^{III} (see Supporting Information for examples of spectra), as observed in our previous work. The HR-ESI-MS of the biscarbene **5a** did not show any peaks with masses higher than lysozyme or cytochrome c, respectively, that might have been assigned to metal complex adducts. Again, this is in line with previous observations where cationic Ir^I complexes did not show any protein binding. However unlike all previous bis(carbene) complexes, compounds **6** with thiazole ligands did show clearly discernible interactions with the two model proteins (Figure 2).

For the interaction of **6a** with lysozyme only one relevant peak is observed at 15062.6 Da, while for **6b**, two additional peaks at 14915.0 and 15025.9 Da appear after incubation of the metal complex with lysozyme. The formation of additional peaks was also observed after treatment of cytochrome c with these complexes. Unfortunately, it was not possible to identify any reasonable fragments of the complexes that would fit to the observed *m/z* peaks in the mass spectra.

Interactions with Short Oligonucleotides

Since the iridium bis(carbene) complexes showed no or rather very few identifiable interactions with our model proteins cytochrome c and lysozyme, we sought to gain more information about other possible targets for these complexes.

DNA is a confirmed target for Pt-based anticancer drugs. Their mode of action has been linked to their ability to crosslink purine bases on the DNA which can lead to a significant damage of the DNA resulting in the subsequent induction of apoptosis.

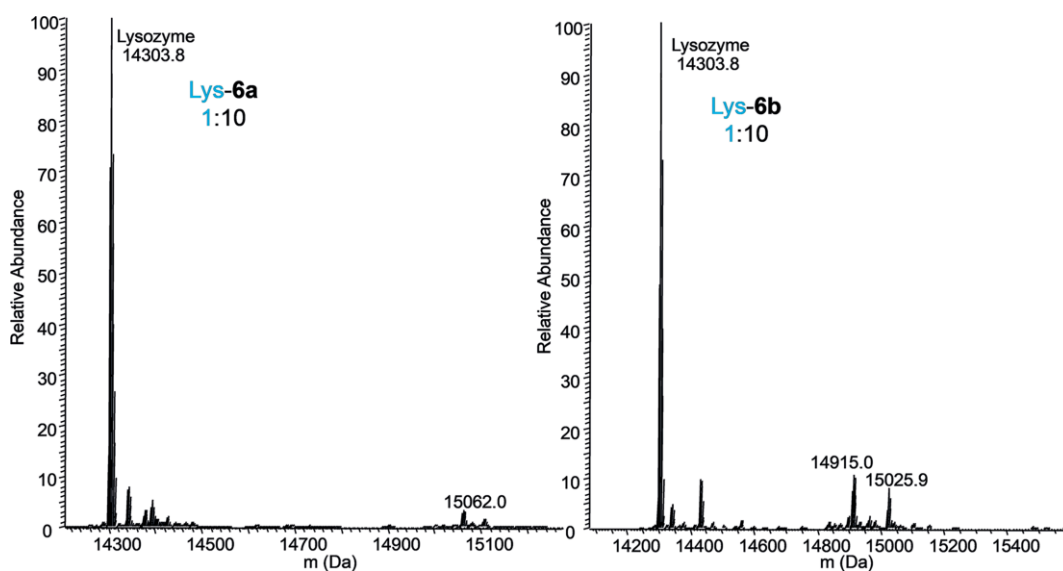


Figure 2. HR-ESI mass spectrum of cytochrome c treated with 1 mM of **6a** (left) or **6b** (right) (complex/protein = 10:1) in 20 mM ammonium acetate buffer (30 % DMSO for **6a**, 10 % DMSO for **6b**), recorded after 72 h of incubation at 37 °C.

To probe DNA as a potential target for the iridium bis(carbene) complexes, their reactivity with DNA was investigated with high resolution electrospray ionization mass spectrometry (HR-ESI-MS) using an oligonucleotide as DNA model system. Oligonucleotides are short nucleic acid polymers, which are used for studying DNA-metal interactions to identify potential nucleobase binding sites. The oligonucleotide used in this study consists of six nucleotides of the bases guanine and cytosine with the sequence 5'-CGCGCG-3', and is abbreviated ODN1 (Figure 3).

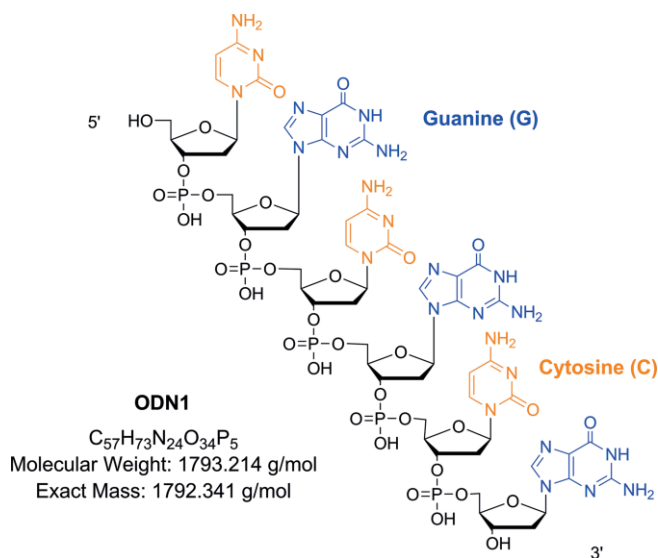


Figure 3. Chemical structure of oligonucleotide ODN1 of sequence 5'-CGCGCG-3'.

The bis(carbene) complexes were incubated with ODN1 in a 3:1 ratio (complex/ODN1) at 37 °C in H₂O and 30 % DMSO for **6a** and 10 % DMSO for all other bis(carbene) complexes. After an incubation time of 24 and 48 h, adduct formation was detected by HR-ESI MS in negative ion mode and with charge states between -2 and -4. In general, no adduct formation was evident for the imidazole and triazole-based complexes **5a** and **7** whereas the thiazole-containing complexes **6a** and **6b** show a well-defined interaction with ODN1. Figure 4 shows the resulting HR-ESI MS spectrum of ODN1 after incubation with compound **6a** for 24 h, the respective data for **6b** are shown in the Supporting Information.

The two signals (blue) at $m/z = 596.43882$ with $z = 3$ and at $m/z = 895.16226$ with $z = 2$ originate from the $[\text{ODN1} - 2\text{H}]^{2-}$ and $[\text{ODN1} - 3\text{H}]^{3-}$ species, respectively. Two additional signals (green) at $m/z = 823.83981$ with $z = 3$ and at $m/z = 1236.26342$ were obtained and identified as one species. The signals of ODN1 and the adduct differ by 683.2 g/mol. This mass difference fits the molecular mass of **6a** after loss of the cyclooctadiene ligand.

For verification, the spectrum resulting from a potential $\text{ODN1} - [\text{Ir}(\text{NSHC})_2]$ adduct was simulated. Both the experimental and calculated isotope patterns for the signal at $m/z = 823.83981$ with $z = 3$ are presented in the Supporting Information. Comparing the isotopic patterns confirms the origin and

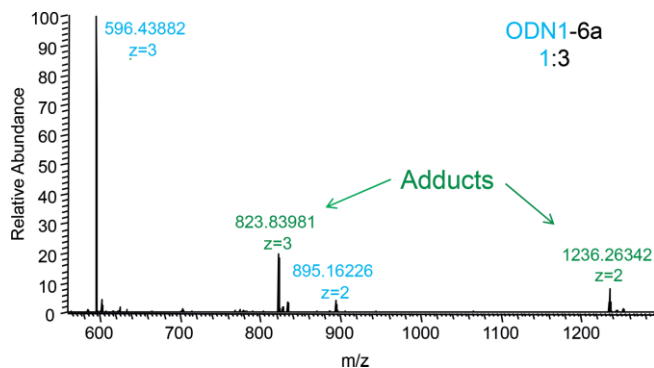


Figure 4. Multicharged ESI mass spectrum of ODN1 incubated with **6a** (1:3) for 24 h at 37 °C.

correct assignment of this signal. Hence it is confirmed that **6a** interacts with ODN1 after or with concomitant loss of its cyclooctadiene ligand. The same binding motif was confirmed for **6b** where the main adduct at $m/z = 774.48708$ with $z = 3$ was assigned to the $\text{ODN1} - [\text{Ir}(\text{NSHC})(\text{NNHC})]$ adduct (see Supporting Information).

Interestingly, from the exact mass and charge of these peaks it can be concluded that the oxidation state of iridium remains unchanged with +I, which is different from the observation of the interactions of monocarbene complexes with proteins from our previous work,^[7e] wherein binding to proteins goes in parallel with an oxidation of the iridium center from +I to +III.

Generation of Reactive Oxygen Species (ROS)

It has previously been shown that redox active metal complexes may be involved in the generation of reactive oxygen species (ROS). ROS are produced in all aerobic cells in a wide range of physiological processes, in particular by mitochondria, playing important roles in signaling transduction.^[11] ROS refer to a group of reactive oxygen radicals, ions or molecules, and they can be categorized into two groups: free oxygen radicals and non-radical ROS. Compared to normal cells, cancer cells already show an increased level of oxidative stress expressed by ROS, partly due to abnormal mitochondrial activity,^[12] in other words, their redox equilibrium is already slightly off balance. It has been shown that an additional increase in ROS levels in cancer cells, through treatment with ROS producing agents, can lead to cell death.^[11c,13a-13d] Therefore, an emerging anticancer strategy is the generation of reactive oxygen species in cancer cells. It is further supposed, that such oxidative stress would have a smaller effect in normal cells, which have an intact redox balance.^[14] In this way, higher cancer selectivity could be achieved with ROS-inducing drug candidates such as redox-active metal complexes.

To see whether the antiproliferative activities of the cytotoxic complexes presented in this work is associated with a ROS-mediated mechanism of action, selected complexes were tested for their ability to produce ROS in MCF-7 cells. A frequently used method for detecting ROS in living cells is the application of fluorescent probes, which are excellent sensors of ROS since they provide a high sensitivity.^[15] In this work, the total ROS

production as well as the production of superoxide has been investigated with a ROS/Superoxide detection kit (Enzo Life Sciences) using flow cytometry. Superoxide is a precursor of most other reactive oxygen species, and further involved in the propagation of oxidative chain reactions.^[16] Two different fluorescent dyes were used; one for total ROS detection [Oxidative Stress Detection Reagent (Green)] and the other one for the detection of superoxide [Superoxide Detection Reagent (Orange)]. The combination of these dyes allows the specification and differentiation of reactive oxygen species (ROS) and superoxide in living cells. Positive controls were obtained using pyocyanin, while negative controls included cells treated only with medium and buffer, and are thus expected to show “normal” signaling levels of ROS/superoxide.

In this work, MCF-7 cells were incubated with equipotent concentrations of our compounds, corresponding to the IC₅₀.

Afterwards, cells were stained with the fluorescent dyes and analyzed by flow cytometry. Table 2 shows the normalized population numbers, and Figure 5 shows selected flow cytometry dot plots, as well as histograms with the different populations observed for compounds **4a** (left), **4bBr** (middle), and **6b** (right).

Additional plots for the other compounds in this study are available in the Supplementary Information. For compound **4a**, a substantial increase in total ROS levels is observed after treatment of the cells compared to untreated cells. Interestingly, the chloride to bromide substitution in **4bBr** leads to a significantly different behavior, in that **4bBr** produces very high amounts of superoxide, with no additional ROS species detectable compared to the control. The bis(carbene) complexes (see Figure 5, right, for **6b** as an example) again show very similar behavior to the monocarbene complex **4a**. In this case, only 1–2 % of

Table 2. Normalized population numbers (%), obtained for Q1–Q4 of the negative control and the complexes **4a**, **4bBr**, **6a**, **b** and **7**. Q1: FL1–/FL2+ (high superoxide), Q2: FL1+/FL2+ (high total oxidative stress and high superoxide), Q3: FL1+/FL2– (high total oxidative stress), Q4: FL1–/FL2– (low oxidative stress and low superoxide). The numbers are reported to two relevant digits (related to the error) in all cases for consistency, thus resulting in apparently different precision.

Sector	Neg. control	4a	4bBr	7	6a	6b
Q1	0.0081 ± 0.0038	5.0 ± 0.14	99.810 ± 0.069	1.720 ± 0.036	7.83 ± 0.32	0.86 ± 0.14
Q2	0.026 ± 0.020	95.0 ± 0.14	0.0102 ± 0.0031	92.28 ± 0.52	91.26 ± 0.36	98.08 ± 0.20
Q3	0.0022 ± 0.0039	0.0250 ± 0.0026	0	4.94 ± 0.59	0.693 ± 0.041	0.970 ± 0.061
Q4	99.965 ± 0.021	0.035 ± 0.014	0.180 ± 0.066	1.060 ± 0.076	0.220 ± 0.070	0.096 ± 0.043

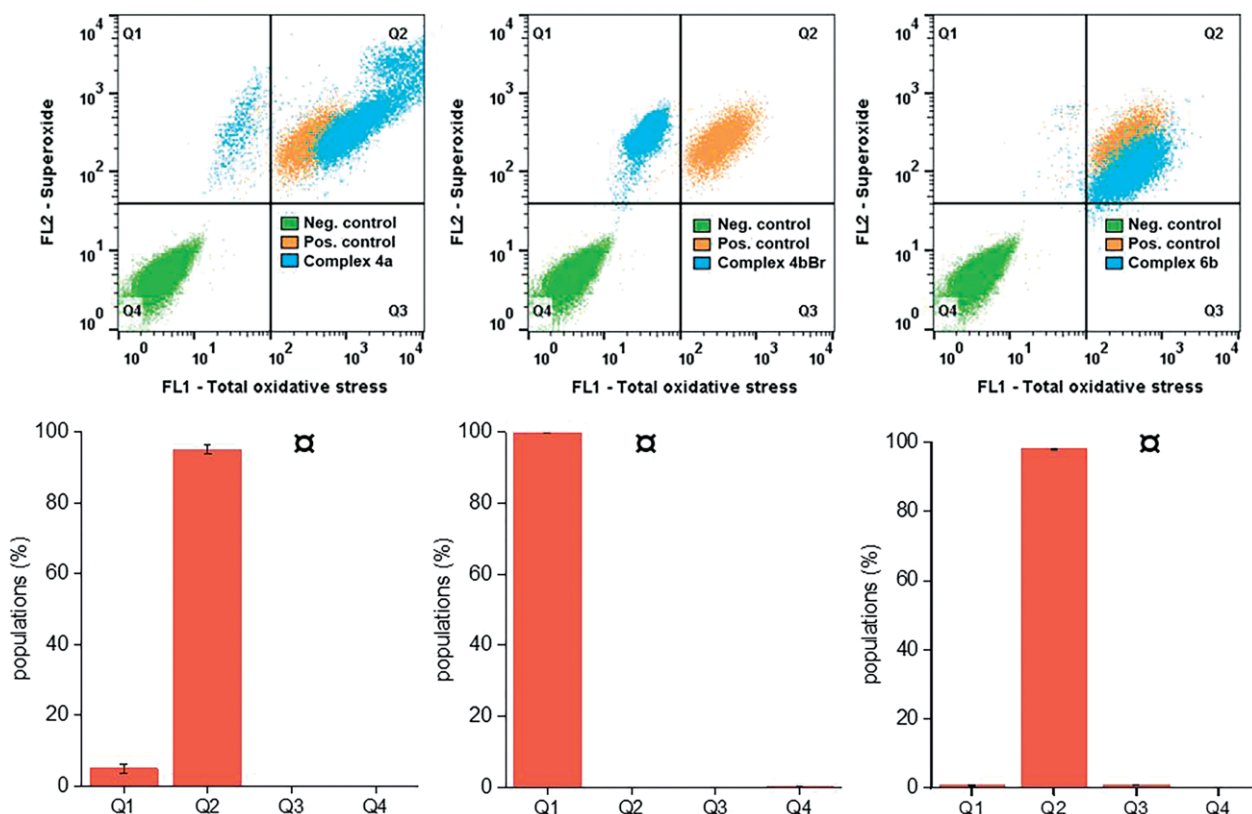


Figure 5. Flow cytometry dot plots and histograms of the different populations observed for **4a** (left), **4bBr** (middle) and **6b** (right).

the total ROS production is related to superoxide (ca. 5 % for **4a**). Of all compounds tested in this work, the bis(carbene) complex **6a** produces the highest amount of total ROS.

Conclusions

In this work, the synthesis, characterization and biological activity of Ir complexes in the +I oxidation state are reported. In comparison to the many Ir^{III} compounds reported in the literature, biological investigations on Ir^I compounds are still relatively rare. The compounds are stabilized by the use of N-heterocyclic carbene-type ligands, namely triazole (NNHC) and thiazole-derived (NSHC) ligands. The synthesis of all compounds follows standard routes, however care has to be taken with the order of addition of carbene ligands in bis(carbene) Ir complexes as not all synthetic routes will lead to the desired products. Namely, thiazole-derived ligands seem to be more labile, and should be added in the last steps only.

In line with this observation about the relative lability of the NSHC ligand in those complexes, significant interactions between the model proteins lysozyme and cytochrome c and the bis(carbene) complexes were only observed for the thiazole-containing complexes **6a**, **b**. Still, the intensity and quantity of the observed peaks was much lower than the monocarbene complexes studied earlier,^[7c,7e] indicating weak protein-metalating ability for the compounds under investigation herein. Among the cationic complexes, only compounds **6** showed interaction with the hexameric oligonucleotide ODN1. Concerning a possible mode of action, it should be noted that Cyt c and lysozyme are just two model proteins, similar to ODN1 being a model nucleotide. While the fact that our compounds do not strongly interact with either model protein or ODN1 seems like an indication against proteins or DNA as the primary target, the possibility that a specific target interaction causes the antiproliferative activity cannot be ruled out completely, e.g. selective inhibition of one particular vital enzyme.

In general, treatment of MCF-7 cells with each of the Ir-NHCs described in this work increased ROS production significantly. Most compounds show a very similar pattern of ROS production with high total amounts of ROS, but only small amounts of superoxide. However, with more than 99 % of total ROS being superoxide, **4bBr** presents a notable exception among all tested compounds. This is even more notable in that **4bBr** does not show any different overall activity in MCF-7 cells (or HT-29 for that matter) from the other related monocarbene compounds. Electrochemistry gives no hint of reversible redox activity of the Ir^I carbene complexes studied herein (see Supporting Information for cyclic voltammograms of two representative examples), so ROS production is likely not caused by a direct ROS-producing catalytic mechanism involving the metal complexes, but rather a downstream cellular response.

We thus conclude that despite the electronic analogy between the d⁸-Pt^{II} and d⁸-Ir^I systems, at least for the organometallic, NHC-derived metal complexes studied in this work, very different mechanisms seem to be responsible for their antiproliferative activity. A first indication might be the fact that ROS production increases dramatically, and is indeed dependent on

the nature of our Ir compounds in cancerous cells. With regard to target elucidation, Ir^I compounds with NHC-type ligands show promising features, and this class of compounds certainly merits further investigation.

Experimental Section

General: Reactions were carried out under N₂ by using standard Schlenk techniques. All solvents were of analytical grade. Chemicals were obtained from commercial sources and used without further purification. ¹H and ¹³C NMR spectra were recorded at room temperature on Bruker DPX 200, DPX 250 and DRX 400 spectrometers, respectively, in deuterated solvents which were used as internal reference. The chemical shifts are reported in ppm (parts per million) relative to TMS. Coupling constants *J*, are reported in Hz, multiplicities being marked as: singlet (s), doublet (d), triplet (t) or multiplet (m). IR spectra were measured on a Bruker Tensor 27 instrument equipped with an attenuated total reflection (ATR) unit at 4 cm⁻¹ resolution. ESI mass spectra were measured on a Bruker Esquire 6000 mass spectrometer. FAB and EI high resolution mass spectrometry were performed with a Fisons VG Instruments Autospec spectrometer. High-resolution mass spectra were recorded with an LTQ Orbitrap high-resolution mass spectrometer (Thermo Scientific, San Jose, CA, USA) equipped with a conventional ESI source. The mass-to-charge relation (*m/z*) is given as a dimensionless number. UV/Vis absorption spectra were recorded on a Varian Cary 50 spectrophotometer. Absorption maxima λ_{max} are given in nm. Elemental analyses were carried out on a Vario EL (Elementar Analysensysteme GmbH, Hanau, D) in C, H, N mode.

Cell Culture and Cytotoxicity: Dulbecco's Modified Eagle's Medium (DMEM), containing 10 % fetal calf serum, 1 % penicillin and streptomycin, was used as growth medium. MCF-7 and HT-29 cells were detached from the wells with trypsin and EDTA, harvested by centrifugation and resuspended again in cell culture medium. The assays were carried out on 96-well plates with 6000 cells per well for both cell lines, MCF-7 and HT-29. After 24 h of incubation at 37 °C and 10 % CO₂, the cells were treated with the compounds (with DMSO concentrations of 0.5 %) with a final volume of 200 μL per well. For a negative control, one series of cells was left untreated. The cells were incubated for 48 h followed by adding 50 μL MTT (2.5 mg/mL). After an incubation time of 2 h, the medium was removed and 200 μL DMSO were added. The formazan crystals were dissolved and the absorption was measured at 550 nm, using a reference wavelength of 620 nm. Each test was repeated in triplicate or quadruplicate in at least three independent experiments for each cell line.

Interaction with Cytochrome c (Lysozyme): Solutions of the complexes (100 μM) with cytochrome c (lysozyme) (3:1 or 10:1 complex/protein molar ratio) in ammonium acetate buffer (20 μM, pH = 6.8) and a compound-specific percentage of DMSO were incubated at 37 °C. After 24 h (48 h, 72 h) and 20-fold dilution with LC-MS grade water, ESI MS spectra were recorded by direct injection at 5 μL min⁻¹ flow rate in an Orbitrap high-resolution mass spectrometer (Thermo, San Jose, CA, USA), equipped with a conventional ESI source. The working conditions were as follows: spray voltage 3.1 kV, capillary voltage 45 V, capillary temperature 220 °C, tube lens voltage 230 V. The sheath and the auxiliary gases were set, respectively, at 17 (arbitrary units) and 1 (arbitrary units). For acquisition, Xcalibur 2.0. software (Thermo) was used and monoisotopic and average deconvoluted masses were obtained by using the integrated Xtract tool. For spectrum acquisition a nominal resolution (at *m/z* 400) of 100,000 was used.

Interaction with Oligonucleotide ODN1: Solutions of the complexes (100 μM) were incubated with ODN1 (3:1 ratio complex/ODN1) in H_2O and a compound-specific percentage of DMSO at 37 $^\circ\text{C}$. After 24 h (48 h, 72 h) and 20-fold dilution with LC-MS grade water, HR-ESI MS spectra were recorded in negative mode by direct injection at a flow rate 5 $\mu\text{L min}^{-1}$.

ROS and Superoxide Determination: Flow cytometry analyses of ROS/superoxide generation by exposure to the complexes was carried out using the Total ROS/Superoxide detection kit (Enzo life sciences) according to the supplier's instructions. Briefly, 1.0×10^6 MCF-7 cells per well were seeded in a 6-well plate. Cells were pre-incubated in drug-free media at 37 $^\circ\text{C}$ for 24 h in a 5% CO_2 humidified atmosphere, and then drugs were added at equipotent concentrations equal to the IC_{50} value. After 48 h of drug exposure, supernatants were removed by suction and cells were washed and harvested. Staining was achieved in the dark by re-suspending the cell pellets in buffer containing the orange/green fluorescent reagents. Cells were analyzed in a Becton Dickinson FACScan Flow Cytometer using Ex/Em: 490/525 nm for the oxidative stress and Ex/Em: 550/620 nm for superoxide detection. Data were processed using the Flowjo software. Negative controls included untreated cells. Positive controls were obtained using pyocyanin.

Synthesis

The synthesis of compound **7** has been reported previously.^[7e]

1: In a flame-dried Schlenk flask 1-methylimidazole (971 μL , 12.2 mmol) and iodomethane (1.35 mL, 14.6 mmol) were dissolved in dry THF (15 mL) and stirred at room temperature for 2 h. The precipitated solid was washed three times with THF to obtain **1** as a white solid (2.55 mg, 93.4%). $^1\text{H NMR}$ (200 MHz, CD_2Cl_2): δ = 9.08 (s, 1 H, N-CH=N), 7.70 (d, J = 1.6 Hz, 2 H, N-CH=CH-N), 3.85 (s, 6 H, H_{NMe}) ppm. $^{13}\text{C NMR}$ (50 MHz, DMSO): δ = 136.9 (N-CH=N), 123.3 (NCH=CHN), 35.8 (C_{NMe}) ppm. MS (ESI⁺): m/z = 96.8 [M - I]⁺.

2a: 1-(Chloromethyl)-2,3,4,5,6-pentamethylbenzene (804.9 g, 4.09 mmol) and 1-methyl-1,2,4-triazole (365 μL , 4.09 mmol) were dissolved in dry THF (10 mL) and stirred under reflux for 48 h. The precipitated solid was filtered and was washed three times with THF to obtain **2a** as a white solid (843.4 mg, 73.7%). $^1\text{H NMR}$ (250 MHz, CD_2Cl_2): δ = 12.33 (s, 1 H, N-C₅H), 7.98 (s, 1 H, N-C₃H), 5.79 (s, 2 H, N-CH₂), 4.27 (s, 3 H, H_{NMe}), 2.27 (s, 9 H, Me), 2.24 (s, 6 H, Me) ppm. $^{13}\text{C NMR}$ (63 MHz, CD_2Cl_2): δ = 144.9 (N=CH-N), 142.7 (N-CH=N), 138.2 ($\text{C}_{\text{Ar-1}}$), 134.6 ($\text{C}_{\text{Ar-2}}$), 134.1 ($\text{C}_{\text{Ar-3}}$), 125.1 ($\text{C}_{\text{Ar-4}}$), 48.9 (N-CH₂), 40.0 (C_{NMe}), 17.6 (Me), 17.3 (Me), 17.2 (Me) ppm. MS (FAB⁺): m/z = 244.1 [M - Cl]⁺.

2b: To a flame-dried Schlenk flask 2-bromoethyl methyl ether (498 μL , 5.30 mmol) and 1-methyl-1,2,4-triazole (200 μL , 2.65 mmol) were dissolved in dry acetonitrile (5 mL) and stirred under reflux for 96 h. After removal of the solvent under reduced pressure, **2b** was obtained as a colorless liquid (335.5 mg, 57%). $^1\text{H NMR}$ (200 MHz, D_2O): δ = 8.86 (s, 1 H, N-C₃H), 4.52 (t, J = 4.9 Hz, 2 H, N-CH₂), 4.14 (s, 3 H, H_{NMe}), 3.85 (t, J = 4.9 Hz, 2 H, O-CH₂), 3.40 (s, 3 H, H_{OMe}) ppm. $^{13}\text{C NMR}$ (50 MHz, D_2O): δ = 144.7 (N=CH-N), 144.6 (N-CH=N), 69.0 (O-CH₂), 58.2 (C_{OMe}), 47.7 (N-CH₂), 38.6 (C_{NMe}) ppm.

2c: 1-Methyl-1,2,4-triazole (200 μL , 2.65 mmol) and iodomethane (165 μL , 2.65 mmol) were stirred in a flame-dried Schlenk flask. A white solid formed within 5 min. The reaction was continued for another 2 h to ensure complete conversion to the product to give **2c** as white solid (584.4 mg, 98%). The product was used for the next reaction without further purification and characterization.

3a: In a flame-dried Schlenk flask 1-(chloromethyl)-2,3,4,5,6-pentamethylbenzene (1.66 g, 8.46 mmol) and thiazole (600 μL ,

8.46 mmol) were dissolved in dry THF (5 mL) and stirred under reflux for 48 h. The precipitated solid was filtered and washed two times with THF to obtain **3a** as white solid (1.72 g, 72.3%). $^1\text{H NMR}$ (250 MHz, CD_3OD): δ = 8.28 (s, 2 H, S-CH=CH-N), 5.90 (s, 2 H, N-CH₂), 2.30 (s, 3 H, Me), 2.27 (s, 6 H, Me), 2.25 (s, 6 H, Me) ppm. MS (ESI⁺): m/z = 245.8 [M - Cl]⁺.

4a: A Schlenk flask was charged with **2a** (70.0 mg, 250 μmol) and Ag_2O (29.0 mg, 125 μmol) in dry dichloromethane (4 mL) and stirred at r.t for 1 h. Following, 0.5 equiv. of $[\text{Ir}(\text{COD})\text{Cl}]_2$ (84.0 mg, 125 μmol) was added and the resulting mixture was stirred for 24 h. The resulting suspension was filtered through Celite, and the filtrate was concentrated to dryness. The crude product was purified by column chromatography on silica using mixtures of dichloromethane and methanol to obtain **4a** (102 mg, 70.4%) as a yellow solid. $^1\text{H NMR}$ (400 MHz, CD_2Cl_2): δ = 7.20 (s, 1 H, N-C₃H), 5.76 (d, J = 14.5 Hz, 1 H, N-CH₂), 5.35 (d, J = 14.7 Hz, 1 H, N-CH₂), 4.69–4.60 (m, 2 H, COD), 4.10 (s, 3 H, H_{NMe}), 3.17–3.06 (m, 2 H, COD), 2.35–2.26 (m, 4 H, COD), 2.28 (s, 3 H), 2.24 (s, 6 H), 2.22 (s, 6 H), 1.89–1.76 (m, 2 H, COD), 1.76–1.64 (m, 2 H, COD) ppm. $^{13}\text{C NMR}$ (101 MHz, CD_2Cl_2): δ = 183.6 (NCN), 141.3 (C_3), 137.0 ($\text{C}_{\text{Ar-1}}$), 134.2 ($\text{C}_{\text{Ar-2}}$), 134.1 ($\text{C}_{\text{Ar-3}}$), 127.1 ($\text{C}_{\text{Ar-4}}$), 86.7 (COD), 86.5 (COD), 52.7 (COD), 52.1 (COD), 49.0 (N-CH₂), 40.2 (C_{NMe}), 34.3 (COD), 34.0 (COD), 30.2 (COD), 30.0 (COD), 17.5 (Me), 17.2 (Me), 17.1 (Me) ppm. MS (FAB⁺): m/z = 579.1 [M]⁺, 544.1 [M - Cl]⁺, 471.0 [M - COD]⁺.

4b: A Schlenk flask was charged with **2b** (170.0 mg, 765 μmol) and Ag_2O (88.9 mg, 383 μmol) in dry dichloromethane (10 mL) and stirred at r.t for 1 h. Following, 0.5 equiv. of $[\text{Ir}(\text{COD})\text{Cl}]_2$ (257.8 mg, 383 μmol) was added and the resulting mixture was stirred for 12 h. The resulting suspension was filtered through Celite, and the filtrate was concentrated to dryness. The crude product was purified by column chromatography on silica using mixtures of dichloromethane and methanol to obtain **4b** (348 mg, 90.0%) as yellow solid. $^1\text{H NMR}$ (400 MHz, CD_2Cl_2): δ = 8.03 (s, 1 H, N-C₃H), 4.68 (ddd, J = 14.3, 5.1, 3.1 Hz, 1 H, N-CH₂), 4.59 (ddd, J = 10.6, 7.1, 4.1 Hz, 2 H, COD), 4.43 (ddd, J = 14.3, 7.8, 3.6 Hz, 1 H, N-CH₂), 4.08 (s, 3 H, H_{NMe}), 3.83–3.71 (m, 2 H, O-CH₂), 3.35 (s, 3 H, H_{OMe}), 3.02–2.96 (m, 1 H, COD), 2.86 (td, J = 7.1, 3.3 Hz, 1 H, COD), 2.29–2.15 (m, 4 H, COD), 1.82–1.64 (m, 4 H, COD) ppm. $^{13}\text{C NMR}$ (101 MHz, CD_2Cl_2): δ = 183.3 (NCN), 143.6 (C_3), 86.7 (COD), 86.6 (COD), 71.6 (O-CH₂), 59.4 (C_{OMe}), 52.9 (COD), 52.5 (COD), 48.9 (N-CH₂), 39.8 (C_{NMe}), 34.1 (COD), 34.0 (COD), 30.0 (COD), 30.0 (COD) ppm. MS (FAB⁺): m/z = 476.8 [M]⁺. $\text{C}_{14}\text{H}_{23}\text{ClIrN}_3\text{O}$ (477.03): calcd. C 35.25, H 4.86, N 8.81; found C 35.00, H 4.60, N 8.58.

4bBr: Compound **4b** (22.9 mg, 48 μmol) was stirred with 3 equiv. of KBr (17.1 mg, 144 μmol) in acetonitrile for 72 h. The solution was filtered through Celite and evaporated to give **4bBr** (22.1 mg, 88.4%) as a yellow solid. $^1\text{H NMR}$ (400 MHz, CD_2Cl_2): δ = 8.04 (s, 1 H, N-C₃H), 4.72–4.61 (m, 3 H, N-CH₂, COD), 4.41 (ddd, J = 14.3, 8.3, 3.2 Hz, 1 H, N-CH₂), 4.05 (s, 3 H, H_{NMe}), 3.81 (ddd, J = 10.4, 8.2, 2.9 Hz, 1 H, O-CH₂), 3.73 (ddd, J = 10.4, 5.2, 3.2 Hz, 1 H, O-CH₂), 3.35 (s, 3 H, H_{OMe}), 3.01 (td, J = 7.2, 3.6 Hz, 1 H, COD), 2.87 (td, J = 7.0, 2.7 Hz, 1 H, COD), 2.30–2.07 (m, 4 H, COD), 1.85–1.73 (m, 2 H, COD), 1.61–1.54 (m, 2 H, COD) ppm. $^{13}\text{C NMR}$ (101 MHz, CD_2Cl_2): δ = 183.3 (NCN), 143.7 (C_3), 86.1 (COD), 86.0 (COD), 71.4 (O-CH₂), 59.4 (C_{OMe}), 53.8 (COD), 53.3 (COD), 48.8 (N-CH₂), 39.8 (C_{NMe}), 33.8 (COD), 33.7 (COD), 30.4 (COD), 30.2 (COD) ppm. MS (FAB⁺): m/z = 520.9 [M]⁺. $\text{C}_{14}\text{H}_{23}\text{BrIrN}_3\text{O}$ (521.48): calcd. C 32.25, H 4.45, N 8.06; found C 32.33, H 4.16, N 7.94.

4c: In a flame-dried Schlenk flask $[\text{Ir}(\text{COD})\text{Cl}]_2$ (248 mg, 368 μmol) and NaBF_4 (80.7 mg, 735 μmol) were dissolved in acetonitrile (2 mL) and stirred for 30 min at room temperature. Subsequently, **2c** (165 mg, 735 μmol) and KOtBu (82.5 mg, 735 μmol) were added to

the suspension and it was stirred overnight. After removal of the solvent, the crude product was purified by column chromatography on silica using mixtures of dichloromethane and methanol to give **4c** as yellow solid (270 mg, 70.0 %). ¹H NMR (200 MHz, CD₂Cl₂): δ = 7.88 (s, 1 H, N-C₃H), 4.87–4.69 (m, 2 H, COD), 3.99 (s, 3 H, H_{NMe}), 3.84 (s, 3 H, H_{NMe}), 3.09–2.90 (m, 2 H, COD), 2.23–2.08 (m, 4 H, COD), 1.89–1.74 (m, 2 H, COD), 1.47–1.33 (m, 2 H, COD) ppm. ¹³C NMR (50 MHz, CD₂Cl₂): δ = 183.9 (NCN), 143.5 (C₃), 84.7 (COD), 84.6 (COD), 55.9 (COD), 55.4 (COD), 39.7 (C_{NMe}), 35.2 (COD), 33.4 (COD), 33.3 (COD), 30.8 (COD) ppm.

5a: Compound **4a** (20 mg, 34.5 μmol), **1** (7.7 mg, 34.5 μmol) and K₂CO₃ (4.9 mg, 34.5 μmol) were stirred in dry dichloromethane (3 mL) at r.t for 48 h. The resulting suspension was filtered through Celite and the filtrate was concentrated to dryness. The remaining orange oil was purified by column chromatography on silica using mixtures of dichloromethane and methanol to give **5a** (21.9 mg, 82.8 %) as orange solid. ¹H NMR (400 MHz, CD₂Cl₂): δ = 7.28 (s, 1 H, N-C₃H), 7.18 (d, *J* = 3.3 Hz, 2 H, N-CH=CH-N), 5.34 (d, *J* = 13.9 Hz, 1 H, N-CH₂), 5.07 (d, *J* = 13.9 Hz, 1 H, N-CH₂), 4.31–4.23 (m, 1 H, COD), 4.22 (s, 3 H, H_{NMe}), 4.21–4.17 (m, 1 H, COD), 4.10 (s, 3 H, H_{NMe}), 3.87 (d, *J* = 7.6 Hz, 3 H, H_{NMe}), 3.87–3.81 (m, 1 H, COD), 3.80–3.72 (m, 1 H, COD), 2.48–2.37 (m, 2 H, COD), 2.35–2.30 (m, 2 H, COD), 2.27 (s, 3 H, Me), 2.23 (s, 6 H, Me), 2.20–2.15 (m, 2 H, COD), 2.04 (s, 6 H, Me), 1.99–1.91 (m, 2 H, COD) ppm. ¹³C NMR (101 MHz, CD₂Cl₂): δ = 182.0 (NCN_{Triaz}), 176.2 (NCN_{Imidaz}), 142.1 (C₃), 137.9 (C_{Ar-1}), 134.6 (C_{Ar-2}), 133.6 (C_{Ar-3}), 125.8 (C_{Ar-4}), 124.4 (N-CH=CH-N), 123.6 (N-CH=CH-N), 81.5 (COD), 78.3 (COD), 77.8 (COD), 76.9 (COD), 48.9 (N-CH₂), 41.4 (C_{NMe}), 39.1 (C_{NMe}), 38.6 (C_{NMe}), 33.5 (COD), 30.4 (COD), 30.3 (COD), 17.5 (Me), 17.2 (Me), 16.8 (Me) ppm. MS (FAB⁺): *m/z* = 640.1 [M]⁺.

6a: [Ir(COD)Cl]₂ (35.9 mg, 53.5 μmol) and NaBF₄ (11.8 mg, 107 μmol) were dissolved in acetonitrile (2 mL) and stirred for 30 min at room temperature. Subsequently, **3a** (30 mg, 107 μmol) and KO_tBu (12 mg, 107 μmol) were added to the suspension and it was stirred overnight. After removal of the solvent, the crude product was purified by column chromatography on silica using mixtures of dichloromethane and methanol to give **6a** as bright orange solid (72 mg, 44.8 %). ¹H NMR (400 MHz, CD₂Cl₂): δ = 7.49 (d, *J* = 3.8 Hz, 2 H, N-CH=CH-S), 7.12 (d, *J* = 3.9 Hz, 2 H, N-CH=CH-S), 5.69 (s, 4 H, N-CH₂), 4.17 (s, 4 H, COD), 2.55–2.34 (m, 8 H, COD), 2.30 (s, 6 H, Me), 2.25 (s, 12 H, Me), 2.07 (s, 12 H, Me) ppm. ¹³C NMR (101 MHz, CD₂Cl₂): δ = 206.1 (NCN), 138.0 (C_{Ar-1}), 135.7 (N-CH=CH-S), 134.5 (C_{Ar-2}), 133.9 (C_{Ar-3}), 127.2 (C_{Ar-4}), 123.4 (N-CH=CH-S), 87.9 (COD), 56.6 (N-CH₂), 32.5 (COD), 32.4 (COD), 17.6 (Me), 17.2 (Me), 17.0 (Me) ppm. MS (ESI⁺): *m/z* = 682.9 [M – COD – Cl]⁺, 790.9 [M – Cl]⁺. MS (FAB⁺): *m/z* = 682.9 [M – COD – Cl]⁺, 790.9 [M – Cl]⁺.

6b: A Schlenk flask was charged with **4c** (40.0 mg, 76.3 μmol), **3a** (21.5 mg, 76.3 μmol) and K₂CO₃ (10.6 mg, 76.3 μmol) and the mixture was stirred in dry dichloromethane (4 mL) at r.t for 120 h. The resulting suspension was filtered through Celite and the filtrate was concentrated to dryness. The remaining orange oil was purified by column chromatography on silica using mixtures of dichloromethane and methanol to give **6b** (43.9 mg, 84.8 %) as orange solid. ¹H NMR (400 MHz, CD₂Cl₂): δ = 8.66 (s, 1 H, N-C₃H), 7.53 (d, *J* = 3.9 Hz, 1 H, N-CH=CH-S), 7.07 (d, *J* = 3.9 Hz, 1 H, N-CH=CH-S), 5.52 (d, *J* = 14.7 Hz, 1 H, N-CH₂), 5.43 (d, *J* = 14.6 Hz, 1 H, N-CH₂), 4.14 (s, 3 H, H_{NMe}), 4.22–3.95 (m, 4 H, COD), 4.09 (s, 3 H, H_{NMe}), 2.47–2.33 (m, 4 H, COD), 2.29 (s, 3 H, Me), 2.24 (s, 6 H, Me), 2.22–2.11 (m, 4 H, COD), 2.07 (s, 6 H, Me) ppm. ¹³C NMR (101 MHz, CD₂Cl₂): δ = 207.9 (NCN_{Thiaz}), 179.2 (NCN_{Triaz}), 145.7 (C₃), 138.0 (C_{Ar-1}), 135.2 (N-CH=CH-S), 134.5 (C_{Ar-2}), 133.9 (C_{Ar-3}), 127.0 (C_{Ar-4}), 123.9 (N-CH=CH-S), 83.6 (COD), 81.8 (COD), 81.1 (COD), 80.7 (COD), 56.7 (N-CH₂), 40.6

(C_{NMe}), 36.1 (C_{NMe}), 32.5 (COD), 32.4 (COD), 31.6 (COD), 31.6 (COD), 17.6 (Me), 17.2 (Me), 17.1 (Me) ppm. MS (ESI⁺): *m/z* = 642.9 [M – Cl]⁺, 534.9 [M – Cl – COD]⁺.

Acknowledgments

Y. G. thanks Elena Michelucci for measurements and simulations of the ESI-MS spectra. T. M. thanks AIRC-FIRC (Fondazione Italiana per la Ricerca sul Cancro, 3-year Fellowship for Italy Project Code: 18044). The authors also gratefully acknowledge financial support from the European Cooperation in Science and Technology (COST) (COST) action CM1105 (STSM to Y. G.), the Beneficentia Stiftung (Vaduz) and CIRCMSB (Bari, Italy). Further, financial support to Y. G. by the Ruhr University Research School PLUS, funded by Germany's Excellence Initiative [DFG GSC 98/3], the ERC (grant no. 247450) and EPSRC (grant no. EP/F034210/1) for P. J. S. are gratefully acknowledged. Dr. Matthew Reback and Isabelle Daubit (RUB) helped measuring the cyclic voltammograms during the revision of this paper.

Keywords: Carbenes · Iridium · Medicinal chemistry · Metal-based drugs · Protein interactions

- [1] a) B. Lippert, *Cisplatin*, Verlag Helvetica Chimica Acta, Zürich, **1999**; b) D. Wang, S. J. Lippard, *Nat. Rev. Drug Discov.* **2005**, *4*, 307–320; c) Y. W. Jung, S. J. Lippard, *Chem. Rev.* **2007**, *107*, 1387–1407; d) N. Cutillas, G. S. Yellol, C. de Haro, C. Vicente, V. Rodriguez, J. Ruiz, *Coord. Chem. Rev.* **2013**, *257*, 2784–2797; e) T. C. Johnstone, K. Suntharalingam, S. J. Lippard, *Chem. Rev.* **2016**, *116*, 3436–3486.
- [2] a) G. Gasser, I. Ott, N. Metzler-Nolte, *J. Med. Chem.* **2011**, *54*, 3–25; b) G. Gasser, N. Metzler-Nolte, *Curr. Opin. Chem. Biol.* **2012**, *16*, 84–91; c) C. G. Hartinger, N. Metzler-Nolte, P. J. Dyson, *Organometallics* **2012**, *31*, 5677–5685.
- [3] a) K. K.-W. Lo, K. Y. Zhang, *RSC Adv.* **2012**, *2*, 12069–12083; b) L. He, Y. Li, C.-P. Tan, R.-R. Ye, M.-H. Chen, J.-J. Cao, L.-N. Ji, Z.-W. Mao, *Chem. Sci.* **2015**, *6*, 5409–5418.
- [4] a) Y. Geldmacher, M. Oleszak, W. S. Sheldrick, *Inorg. Chim. Acta* **2012**, *393*, 84–102; b) V. Novohradsky, L. Zerzankova, J. Stepankova, A. Kisova, H. Kostrhunova, Z. Liu, P. J. Sadler, J. Kasparkova, V. Brabec, *Metallomics* **2014**, *6*, 1491–1501; c) A. Kumar, A. Kumar, R. K. Gupta, R. P. Paitandi, K. B. Singh, S. K. Trigun, M. S. Hundal, D. S. Pandey, *J. Organomet. Chem.* **2016**, *801*, 68–79; d) M. Graf, Y. Gothe, N. Metzler-Nolte, R. Czerwiec, K. Sünkel, *Inorg. Chim. Acta* **2017**, *463*, 36–43; e) M. Graf, Y. Gothe, N. Metzler-Nolte, K. Sünkel, *Z. Anorg. Allg. Chem.* **2017**, *643*, 306–310; f) M. Graf, Y. Gothe, D. Siegmund, N. Metzler-Nolte, K. Sünkel, *Inorg. Chim. Acta* **2018**, *471*, 265–271.
- [5] a) I. Romero-Canelon, P. J. Sadler, *Inorg. Chem.* **2013**, *52*, 12276–91; b) Z. Liu, P. J. Sadler, *Acc. Chem. Res.* **2014**, *47*, 1174–85.
- [6] a) P. K. Sasmal, C. N. Streu, E. Meggers, *Chem. Commun.* **2013**, *49*, 1581–1587; b) see ref.^[5b] c) J. J. Soldevila-Barreda, P. J. Sadler, *Curr. Opin. Chem. Biol.* **2015**, *25*, 172–183; d) P. Zhang, P. J. Sadler, *Eur. J. Inorg. Chem.* **2017**, 1541–1548.
- [7] a) J. Rajput, J. R. Moss, A. T. Hutton, D. T. Hendricks, C. E. Arendse, C. Imrie, *J. Organomet. Chem.* **2004**, *689*, 1553–1568; b) P. V. Simpson, C. Schmidt, I. Ott, H. Bruhn, U. Schatzschneider, *Eur. J. Inorg. Chem.* **2013**, *2013*, 5547–5554; c) Y. Gothe, T. Marzo, L. Messori, N. Metzler-Nolte, *Chem. Commun.* **2015**, *51*, 3151–3153; d) P. V. Simpson, K. Radacki, H. Braunschweig, U. Schatzschneider, *J. Organomet. Chem.* **2015**, *782*, 116–123; e) Y. Gothe, T. Marzo, L. Messori, N. Metzler-Nolte, *Chem. Eur. J.* **2016**, *22*, 12487–94.
- [8] Y. Kondo, S. Izawa, S. Kusabayashi, *J. Chem. Soc., Perkin Trans. 2* **1988**, 1925–1928.
- [9] a) H. V. Huynh, N. Meier, T. Pape, F. E. Hahn, *Organometallics* **2006**, *25*, 3012–3018; b) I. Piel, M. D. Pawelczyk, K. Hirano, R. Froehlich, F. Glorius, *Eur. J. Org. Chem.* **2011**, *2011*, 5475–5484, S5475/1–S5475/132.

- [10] L. Messori, T. Marzo, R. N. Sanches, R. Hanif Ur, D. de Oliveira Silva, A. Merlino, *Angew. Chem. Int. Ed.* **2014**, *53*, 6172–6175; *Angew. Chem.* **2014**, *126*, 6286.
- [11] a) G. Waris, H. Ahsan, *J. Carcinog.* **2006**, *5*, 14–14; b) G.-Y. Liou, P. Storz, *Free Radical Res.* **2010**, *44*, <https://doi.org/10.3109/10715761003667554>; c) Z. Liu, I. Romero-Canelón, B. Qamar, J. M. Hearn, A. Habtemariam, N. P. E. Barry, A. M. Pizarro, G. J. Clarkson, P. J. Sadler, *Angew. Chem. Int. Ed.* **2014**, *53*, 3941–3946; *Angew. Chem.* **2014**, *126*, 4022.
- [12] L. Tong, C.-C. Chuang, S. Wu, L. Zuo, *Cancer Lett.* **2015**, *367*, 18–25.
- [13] a) T. Ozben, *J. Pharm. Sci.* **2007**, *96*, 2181–2196; b) Y. Yang, S. Karakhanova, J. Werner, A. V. Bazhin, *Curr. Med. Chem.* **2013**, *20*, 3677–3692; c) R. Judit, M. Paolo, B. Jacint, *Curr. Drug Targets* **2015**, *16*, 31–37; d) I. Yousuf, F. Arjmand, S. Tabassum, L. Toupet, R. A. Khan, M. A. Siddiqui, *Dalton Trans.* **2015**, *44*, 10330–10342.
- [14] R. A. Cairns, I. S. Harris, T. W. Mak, *Nat. Rev. Cancer* **2011**, *11*, 85–95.
- [15] A. Casini, L. Messori, *Curr. Top. Med. Chem.* **2011**, *11*, 2647–2660.
- [16] J. F. Turrens, *J. Physiol.* **2003**, *552*, 335–344.

Received: February 16, 2018